Convolutive Sparse Decomposition in Inverse Problems: A Sensor Space Approach

Jean-Baptiste Malagnoux, Matthieu Kowalski
Laboratoire Interdisciplinaire des Sciences du Numériques
Inria, Université Paris-Saclay, CNRS
Gif-sur-Yvette, France
{jean-baptiste.malagnoux,matthieu.kowalski}@universite-paris-saclay.fr

***Abstract*—We propose a novel approach that applies convolutional dictionary learning (CDL- decomposition directly in the sensor domain before solving the inverse problem, contrasting it with the classical approach where the inverse problem is solved first. This method enhances computational efficiency and improves spatial localization accuracy, especially when he sources activity is sparse. Theoretically, we establish a formal equivalence between CDL decomposition in the source and sensor domains, laying the groundwork for a practical transition between these two approaches. Using synthetic data, we compare two approaches: (1) resolving the inverse problem first and then performing CDL decomposition, and (2) initially decomposing in the sensor domain, followed by solving the inverse problem on the spatial dictionary. Our results show that the second approach offers improved reconstruction quality and reduced computational costs, making it a promising strategy for addressing complex inverse problems.**

***Index Terms*—inverse problem, convolutive sparse coding, low rank decomposition.**

I. Introduction

Inverse problems have a wide range of applications, including source reconstruction in acoustics [1], medical imaging [2], and computer vision [3]. This article will focus on solving inverse problems using low-rank decomposition and dictionary learning. Low-rank decomposition is an important category of signal processing methods, including techniques like principal component analysis (PCA) [4], robust, sparse PCA, and non-negative matrix factorization (NMF) [5]–[7]. The latter has improved upon interpretability. These methods are used in hyperspectral unmixing [8], recommendation systems often referred to as the Netflix problem [9], and inverse problems, notably for source separation in audio signals [1] and magneto/electroencephalography (M/EEG) studies [10]. While traditional dictionaries with fixed waveforms –such as wavelets or time-frequency atoms– in signal analysis may only capture certain types of events within the data, dictionary learning methods, such as NMF in Gabor domains or convolutional dictionary learning (CDL) [11], are well-suited for inverse problems. For example, in [10], the authors proposed tackling the M/EEG inverse problem using a CDL decomposition in the sensor space, focusing on learning temporal features and brain activities. Then, to localize the different sources, they employed dipole fitting methods [12]. Building on this model, we explore whether a CDL decomposition could be directly applied in the source space. We analyze the relationship between CDL decomposition in the source space versus the sensor space and investigate the transition between the two.

Contributions and outline: After a brief reminder of the inverse problem and on multivariate CDL methods in Section II, we introduce the model for decomposing the data in the source domain in Section III. Then, Thm. 1 establishes the equivalence between decomposition in the source domain after solving the inverse problem versus solving the inverse problem on the spatial dictionary found through decomposition in the sensor space. Next, we present the algorithm to solve our proposed method. Finally, in Section IV, we illustrate our method and its competitiveness through numerical experiments on synthetic data.

Notations: Vectors will be denoted using bold lowercase and matrix in bold uppercase. The element at i-th rows and j-th column of a matrix $\mathbf{M}$ will be denoted by $M[i,j]$, while $\mathbf{M}[i,:]$ denotes the i-th rows and $\mathbf{M}[:,j]$ the j-th column. Similarly, the i-th coordinate of a vector $\mathbf{v}$ will be denoted by $v[i]$. We define the operator $(\cdot)^+$ as $\max(0,\cdot)$. We also denote by $\odot$ the element-wise multiplication between two matrices/vectors of the same dimension. We consider circular convolution between a filter $\mathbf{d} \in \mathbb{R}^L$ and a signal $\mathbf{z} \in \mathbb{R}^T$ denoted by $\mathbf{d} * \mathbf{z} \in \mathbb{R}^T$, where L $\ll$ T. To perform this operation, the filter $\mathbf{d}$ is zero-padded to length T. Since $\mathbf{d}$ is zero-padded to length T prior to the operation, we will regard $\mathbf{d} \in \mathbb{R}^T$ for the sake of notation. The multivariate circular convolution between $\mathbf{z} \in \mathbb{R}^T$ and $\mathbf{D} \in \mathbb{R}^{P\times T}$ is denoted $\mathbf{D} * \mathbf{z} = \begin{pmatrix} \mathbf{d}_1 * \mathbf{z} \\ \vdots \\ \mathbf{d}_P * \mathbf{z} \end{pmatrix} \in \mathbb{R}^{P\times T}$ and is obtained by convolving each row of $\mathbf{D}$ with $\mathbf{z}$.

II. State of the art

This section briefly presents the considered linear inverse problems and state-of-the-art on multivariate convolutional dictionary learning.

A. Inverse problem

We consider the inverse problem where data are obtained from a limited number P of sensors. The temporal duration of

This work was supported by the French National Agency for Research through the BMWs project (ANR-20-CE45-0018)

sensor data acquisition is represented by T, while N denotes the number of sources one might wish to reconstruct. This leads to the following standard formulation of the inverse problem [13]:

$$\mathbf{M} = \mathbf{G}\mathbf{X} + \mathbf{E} \ , \tag{1}$$

where the rows of $\mathbf{M} \in \mathbb{R}^{P\times T}$ correspond to the temporal acquisitions from the sensors. The rows of $\mathbf{X} \in \mathbb{R}^{N\times T}$ represent the temporal activities of the different sources. $\mathbf{G} \in \mathbb{R}^{P\times N}$ is the lead-field matrix, which facilitates the projection between the sources' activities and the sensors' acquisitions. $\mathbf{E} \in \mathbb{R}^{P\times T}$ is an additive white noise.

Equation (1) cannot be solved directly due to the non-invertibility of $\mathbf{G}$. Consequently, regularized optimization problems are employed to estimate the source activity [13]. One possible approach involves utilizing a resolution with time-frequency dictionaries while incorporating a sparse prior [14], highlighting the challenges associated with dictionary selection and representation estimation.

While Gabor or wavelet dictionaries are well-suited for linear analysis, they may face difficulties capturing certain 'non-rhythmic events' that occur in the brain [15], [16]. To tackle this issue, one potential solution is to learn the dictionary directly from the data. This article will specifically focus on Convolutional Dictionary Learning (CDL) [17].

B. Multivariate convolutional dictionary learning

The CDL approach has yielded excellent results in many fields, such as image processing [18], [19] and audio signals [20]. We recall the definition of the multivariate CDL model as proposed by Wohlberg [21].

Definition 1 (Multivariate CDL)**.** *Let* $\mathbf{M} \in \mathbb{R}^{P\times T}$, $\{\mathbf{D}_k\}_{k=1}^K \in \mathbb{R}^{P\times T}$, *and* $\{\mathbf{z}_k\}_{k=1}^K \in \mathbb{R}_+^T$. *We say that* $\mathbf{M}$ *admits a CDL decomposition if it can be expressed as*

$$\mathbf{M} = \sum_{k=1}^K \mathbf{D}_k * \mathbf{z}_k \ . \tag{2}$$

The primary advantage of this decomposition lies in its high interpretability. Specifically, $\mathbf{D} = \{\mathbf{D}_k\}_{k=1}^K \in \mathbb{R}^{P\times T}$ represents the spatio-temporal dictionary, while $\mathbf{z} = \{\mathbf{z}_k\}_{k=1}^K \in \mathbb{R}_+^T$ corresponds to their activations over time. To achieve such a decomposition, Wohlberg proposed solving the following optimization problem:

$$\min_{\mathbf{D},\mathbf{z}} \frac{1}{2}\|\mathbf{M} - \sum_{k=1}^K \mathbf{D}_k * \mathbf{z}_k\|_2^2 + \lambda \sum_{k=1}^K \|\mathbf{z}_k\|_1 \quad \text{s.t. } \|\mathbf{D}_k\|_2^2 \leq 1, \mathbf{z}_k \geq 0 \tag{3}$$

This model has been applied to 3-channel images. In our case, we adopt a variant that imposes a rank-1 constraint on the spatio-temporal atoms, as proposed in [10], [22] for M/EEG data: $\forall, k \in [\![1, K]\!]$, $\mathbf{D}_k = \mathbf{u}_k\mathbf{v}_k^\top$, where $\{\mathbf{u}_k\}_{k=1}^K \in \mathbb{R}^P$ and $\{\mathbf{v}_k\}_{k=1}^K \in \mathbb{R}^T$ denote the spatial and temporal atoms, respectively. We summarize this model in the following definition.

Definition 2 (Rank-1 Multivariate CDL)**.** *We say that* $\mathbf{M}$ *admits a rank-1 CDL decomposition if it exists* $\mathbf{u} = \{\mathbf{u}_k\}_{k=1}^K$, $\mathbf{v} = \{\mathbf{v}_k\}_{k=1}^K$ *and* $\mathbf{z} = \{\mathbf{z}_k\}_{k=1}^K$ *such that:*

$$\mathbf{M} = \sum_{k=1}^K \left(\mathbf{u}_k\mathbf{v}_k^\top\right) * \mathbf{z}_k \ . \tag{4}$$

To achieve such a decomposition, one can solve the following optimization problem [10]:

$$\min_{\mathbf{u},\mathbf{v},\mathbf{z}} \frac{1}{2}\|\mathbf{M} - \sum_{k=1}^K (\mathbf{u}_k\mathbf{v}_k^\top) * \mathbf{z}_k\|_2^2 + \lambda \sum_{k=1}^K \|\mathbf{z}_k\|_1 \quad \text{s.t. } \|\mathbf{u}_k\|_2^2 \leq 1, \|\mathbf{v}_k\|_2^2 \leq 1, \mathbf{z}_k \geq 0 \ . \tag{5}$$

This optimization problem can be solved using alternating minimization with respect to $\mathbf{u}, \mathbf{v}$ and $\mathbf{z}$ [11], [23]. The minimization with respect to $\mathbf{z}$ corresponds to a LASSO problem [24] or Basis Pursuit Denoising [25] which can be efficiently solved by FISTA [26].

III. CDL DECOMPOSITION: FROM THE SOURCES TO THE SENSORS

This section presents our modelizations of the inverse problem as a CDL decomposition directly on the source domain.

A. Theoretical analysis

Assuming that the source domain admits a CDL decomposition, Thm. 1 shows that the sensor data also admits a decomposition of the same form, sharing the same temporal atoms and activations. Moreover, the spatial source atoms can be recovered by solving an inverse problem on the spatial dictionary derived from the sensors.

Theorem 1. *Suppose* $\mathbf{X} \in \mathbb{R}^{N\times T}$ *admits a rank-1 CDL decomposition. That is, it exists* $\tilde{\mathbf{u}} = \{\mathbf{u}_k\}_{k=1}^K$, $\mathbf{v} = \{\mathbf{v}_k\}_{k=1}^K$ *and* $\mathbf{z} = \{\mathbf{z}_k\}_{k=1}^K$ *such that* $\mathbf{X} = \sum_{k=1}^K \left(\tilde{\mathbf{u}}_k\mathbf{v}_k^\top\right) * \mathbf{z}_k$. *Let* $\mathbf{G} \in \mathbb{R}^{P\times N}$ *such that* $\mathbf{M} = \mathbf{G}\mathbf{X}$, *then* $\mathbf{M}$ *also admits a rank-1 CDL decomposition:*

$$\mathbf{M} = \sum_{k=1}^K \left(\mathbf{u}_k\mathbf{v}_k^\top\right) * \mathbf{z}_k \ ,$$

with $\mathbf{u}_k = \mathbf{G}\tilde{\mathbf{u}}_k \ \forall k$.

Proof. We have

$$\mathbf{M} = \mathbf{G}\mathbf{X} = \sum_{k=1}^K \mathbf{G}\left((\tilde{\mathbf{u}}_k\mathbf{v}_k^T) * \mathbf{z}_k\right) \ . \tag{6}$$

Let $\mathbf{W}_k = (\tilde{\mathbf{u}}_k\mathbf{v}_k^\top) * \mathbf{z}_k$. By remarking that one has $\mathbf{W}_k[j,:] = \tilde{u}_k[j]\mathbf{v}_k^\top * \mathbf{z}_k$, we get

$$\mathbf{M}[i,:] = \sum_{k=1}^K \sum_{j=1}^N G[i,j]\mathbf{W}_k[j,:] = \sum_{k=1}^K \sum_{j=1}^N G[i,j]\tilde{u}_k[j]\mathbf{v}_k^\top * \mathbf{z}_k \tag{7}$$

$$= \sum_{k=1}^K \left[\sum_{j=1}^N G[i,j]\tilde{u}_k[j]\mathbf{v}_k^\top\right] * \mathbf{z}_k \tag{8}$$

In the end, we can write

$$\mathbf{M} = \sum_{k=1}^{K} \left((\mathbf{G}\tilde{\mathbf{u}}_k)\mathbf{v}_k^\top \right) * \mathbf{z}_k = \sum_{k=1}^{K} (\mathbf{u}_k \mathbf{v}_k^\top) * \mathbf{z}_k \ . \tag{9}$$

□

Hence, $\mathbf{M}$ can also be expressed as a rank-1 convolutional decomposition which shares the same temporal activations $\mathbf{z}$ and temporal atoms $\mathbf{v}$ as $\mathbf{X}$, while its spatial atoms are given by $\mathbf{u}_k = \mathbf{G}\tilde{\mathbf{u}}_k$.

Furthermore, the converse is true: if $\mathbf{M}$ admits a rank-1 CDL decomposition such that $\mathbf{M} = \sum_{k=1}^{K} \left(\mathbf{u}_k \mathbf{v}_k^\top\right) * \mathbf{z}_k$, and if $\mathbf{G}$ is a full-rank matrix, then it exists $\tilde{\mathbf{u}}_k$ such that $\mathbf{u}_k = \mathbf{G}\tilde{\mathbf{u}}_k$. That is, it exists $\mathbf{X} = \sum_{k=1}^{K} \left(\tilde{\mathbf{u}}_k \mathbf{v}_k^\top\right) * \mathbf{z}_k$ which admit a rank-1 CDL decomposition such that $\mathbf{M} = \mathbf{G}\mathbf{X}$.

B. Optimization implications

Assuming that both spatial localization in the source domain and temporal activities are sparse, one may want to solve the following multi-objective optimization problem [27]

$$\min_{\tilde{\mathbf{u}},\mathbf{v},\mathbf{z}} \left(\sum_{k=1}^{K} \|\mathbf{z}_k\|_1, \sum_{k=1}^{K} \|\tilde{\mathbf{u}}_k\|_1 \right) \tag{10}$$

$$\text{s.t.} \begin{cases} \mathbf{M} = \mathbf{G}\mathbf{X}, \mathbf{X} = \sum_{k=1}^{K} (\tilde{\mathbf{u}}_k \mathbf{v}_k^\top) * \mathbf{z}_k \\ \|\tilde{\mathbf{u}}_k\|_2^2 \leq 1, \|\mathbf{v}_k\|_2^2 \leq 1, \mathbf{z}_k \geq 0, \tilde{\mathbf{u}}_k \geq 0 \end{cases}$$

As a consequence of Thm. 1, the following corollary demonstrates that the optimization problem below leads to a Pareto optimal solution of the problem Eq. (10).

Corollary 1. *Suppose $\mathbf{X} \in \mathbb{R}^{N \times T}$ admits a rank-1 CDL decomposition. That is, it exist $\tilde{\mathbf{u}} = \{\mathbf{u}_k\}_{k=1}^K$, $\mathbf{v} = \{\mathbf{v}_k\}_{k=1}^K$ and $\mathbf{z} = \{\mathbf{z}_k\}_{k=1}^K$ such that $\mathbf{X} = \sum_{k=1}^{K} \left(\tilde{\mathbf{u}}_k \mathbf{v}_k^\top\right) * \mathbf{z}_k$. Let $\mathbf{M} = \mathbf{G}\mathbf{X}$ with $\mathbf{G}$ a full rank matrix. Let*

$$(\mathbf{u}^*, \mathbf{v}^*, \mathbf{z}^*) = \underset{\mathbf{u},\mathbf{v},\mathbf{z}_k}{\operatorname{argmin}} \sum_{k=1}^{K} \|\mathbf{z}_k\|_1 \tag{11}$$

$$s.t.\ \mathbf{M} = \sum_{k=1}^{K} (\mathbf{u}_k \mathbf{v}_k^\top) * \mathbf{z}_k, \|\mathbf{u}_k\|_2^2 \leq 1, \|\mathbf{v}_k\|_2^2 \leq 1, \mathbf{z}_k \geq 0$$

and let

$$\tilde{\mathbf{u}}^* = \underset{\tilde{\mathbf{u}}}{\operatorname{argmin}} \sum_{k=1}^{K} \|\tilde{\mathbf{u}}_k\|_1 \quad s.t.\ \mathbf{u}_k^* = \mathbf{G}\tilde{\mathbf{u}}_k, \tilde{\mathbf{u}}_k \geq 0, \tag{12}$$

Then, $(\tilde{\mathbf{u}}^*, \mathbf{v}^*, \mathbf{z}^*)$ is a Pareto optimal solution of Eq. (10)

Proof. Let $(\mathbf{u}^*, \mathbf{v}^*, \mathbf{z}^*)$ be a global minimizer of Eq. (11) and $\tilde{\mathbf{u}}^*$ a global minimizer of Eq. (12). Let $(\tilde{\mathbf{u}}^\dagger, \mathbf{v}^\dagger, \mathbf{z}^\dagger)$ be a Pareto optimum of Eq. (10). Let $\mathbf{u}^\dagger = \mathbf{G}\tilde{\mathbf{u}}^\dagger$, so according to Thm. 1:

$$\mathbf{M} = \sum_{k=1}^{K} (\mathbf{u}_k^\dagger \mathbf{v}_k^{\dagger\top}) * \mathbf{z}_k^\dagger = \mathbf{G} \sum_{k=1}^{K} (\tilde{\mathbf{u}}_k^\dagger \mathbf{v}_k^{\dagger\top}) * \mathbf{z}_k^\dagger \ , \tag{13}$$

hence $(\mathbf{u}^\dagger, \mathbf{v}^\dagger, \mathbf{z}^\dagger)$ is a feasible point of Eq. (11) and $(\tilde{\mathbf{u}}^\dagger)$ a feasible point of Eq. (12). Consequently, we have

$$\sum_{k=1}^{K} \|\mathbf{z}_k^*\|_1 \leq \sum_{k=1}^{K} \|\mathbf{z}_k^\dagger\|_1 \text{ and } \sum_{k=1}^{K} \|\tilde{\mathbf{u}}_k^*\|_1 \leq \sum_{k=1}^{K} \|\tilde{\mathbf{u}}_k^\dagger\|_1 \tag{14}$$

hence the conclusion. □

A numerical consequence of Corollary 1, illustrated in the next section, is that applying a rank-1 CDL decomposition in the sensor domain, followed by solving the inverse problem on the spatial dictionary, leads to lower computational cost than the reverse order. This gain in efficiency is due to:

- **Reduced problem size:** Since $P < N$, CDL on the sensor data ($P \times T$) is faster than on the source space ($N \times T$).
- **Cheaper inverse step:** Solving K inverse problems of size $P \times N$ on a low-rank spatial dictionary is less demanding than the one on full sensor data of size $P \times (N \times T)$ when $K << N$.

IV. Numerical results

To demonstrate the advantages of the proposed approach, we simulate sparse temporal activations $\mathbf{z}_k \in \mathbb{R}^T$ (and spatial activations $\tilde{\mathbf{u}}_k \in \mathbb{R}^N$) following a Bernoulli-Gaussian model [28] with parameters $p_{\text{temporal}} = 0.01$ (resp. $p_{\text{spatial}} = 0.2$) and $\sigma_{\text{temporal}} = \sigma_{\text{spatial}} = 1$, where $N = 20$ and $T = 10000$. We select $K = 3$ temporal atoms $\mathbf{v}_k \in \mathbb{R}^T$ with an original support of size $L = 128$ and then 0-padded to a size T, as illustrated in red in Fig. 1. We then generate $\mathbf{X} = \sum_{k=1}^{K} \tilde{\mathbf{u}}_k \mathbf{v}_k^\top * \mathbf{z}_k$ and subsequently compute $\mathbf{M} = \mathbf{G}\mathbf{X} + \mathbf{E}$ for various $\mathbf{G} \in \mathbb{R}^{P \times N}$, with $P = 10$ and varying levels of white Gaussian noise to achieve input Signal to Noise Ratios (iSNR) of 5, 10, and 20 dB. The operator $\mathbf{G}$ is a random centered Gaussian matrix with a covariance matrix $\mathbf{C}$ defined such that $C[i,j] = w^{|i-j|}$, where $w \in [0, 1[$.

We then compare the two following approaches

1) **IPFirst:** We first solve the inverse problem Eq. (1) using a structured sparse prior in the time-frequency domain to estimate $\mathbf{X}$ following [14]. Then, we apply a rank-1 CDL decomposition to $\mathbf{X}$ by solving (5). We use a Hann window of length $2L = 256$ with 50% overlap for the time-frequency dictionary. The procedure is summarized in Alg. 1. The hyper-parameters μ_1 and μ_2 are tuned to maximize the output SNR of the estimated $\mathbf{X}$.
2) **CDLFirst:** We first solve the rank-1 CDL decompositions in the sensor doamin on $\mathbf{M}$ by solving (5), and then we solve the sparse inverse problem (12). The procedure is summarized in Alg. 2. The hyper-parameters λ when solving Eq. (5) is tuned to maximize the estimated $\mathbf{X}$ output SNR.

In both methods, we initialize the temporal atoms of the CDL decomposition based on a Nonnegative Matrix Factorization of the spectrograms, following [29], using the same parameters as in IPFirst.

To compare the two methods, we evaluated the quality of the overall data reconstruction using the SNR of the estimated

Quantitative results		oSNR Temporal atoms			Spatial atoms optimal transport			oSNR reconstruction		
Correlation w	**Methods**	**iSNR=5**	**iSNR=10**	**iSNR=20**	**iSNR=5**	**iSNR=10**	**iSNR=20**	**iSNR=5**	**iSNR=10**	**iSNR=20**
0	IPFirst	8.47	10.23	11.35	6.03	6.08	4.18	8.47	15.84	21.23
	CDLFirst	**9.55**	**11.57**	**12.94**	**5.98**	**3.59**	**1.34**	**16.43**	**24.65**	**33.68**
0.8	IPFirst	8.63	11.64	12.47	8.73	7.10	6.81	11.7	14.01	24.37
	CDLFirst	**9.43**	**11.82**	**13.97**	**7.23**	**5.04**	**4.52**	**17.52**	**19.76**	**22.03**
0.99	IPFirst	8.93	11.34	11.41	11.41	10.6	9.54	10.89	**20.82**	**26.23**
	CDLFirst	**9.27**	**12.24**	**12.15**	**10.06**	**9.5**	**8.35**	**12.37**	17.43	23.1

TABLE I

QUANTITATIVE COMPARISON OF THE IPFIRST AND CDLFIRST APPROACHES IN VARIOUS SCENARIOS. IPFIRST AND CDLFIRST ARE COMPARED REGARDING THE OSNR OF THE TEMPORAL ATOMS $\mathbf{v}$, UP TO A GLOBAL PHASE SHIFT (THE HIGHER, THE BETTER), THE WASSERSTEIN DISTANCE OF THE SPATIAL ATOMS $\tilde{\mathbf{u}}$ (THE LOWER, THE BETTER), AND THE OSNR OF THE GLOBAL RECONSTRUCTION OF THE SOURCES $\mathbf{X}$ (THE HIGHER, THE BETTER). THE BEST RESULTS ARE IN BOLD.

Algorithm 1: IPFirst: solving the inverse problem first, then the CDL.

Input : $y \in \mathbb{R}^T$ an observed signal **Result:** $\mathbf{X}$, $\tilde{\mathbf{u}}$, $\mathbf{z}$, $\mathbf{v}$
Estimate $\mathbf{X}$ by solving:
$\mathbf{X} = \mathbf{\Phi}\,\text{argmin}\,\frac{1}{2}\|\mathbf{M} - \mathbf{G}\mathbf{\Phi}\boldsymbol{\alpha}\|_2^2 + \mu_1\|\boldsymbol{\alpha}\|_{21} + \mu_2\|\alpha\|_1$;
where $\mathbf{\Phi}$ is a time-frequency dictionary;
Estimate $\tilde{\mathbf{u}}, \mathbf{v}, \mathbf{z}$ by solving Eq. (5) on $\mathbf{X}$ with $\lambda \to 0$;

Algorithm 2: CDLFirst: solving the CDL first, then the inverse problem.

Result: $\mathbf{X}$, $\tilde{\mathbf{u}}$, $\mathbf{z}$, $\mathbf{v}$
Estimate $\mathbf{u}, \mathbf{v}, \mathbf{z}$ by solving Eq. (5) on $\mathbf{M}$.
Estimate $\tilde{\mathbf{u}}$ by solving Eq. (12)
Estimate $\mathbf{X} = \sum_{k=1}^{K} \tilde{\mathbf{u}}_k \mathbf{v}_k^T * \mathbf{z}_k$

sources. The temporal atoms' recovery quality $\mathbf{v}$ is evaluated using the SNR up to a global phase shift. The SNR being too sensitive to an estimation error in the support for the spatial atoms $\tilde{\mathbf{u}}$, we propose to use the Wasserstein distance between the true atoms and the estimated ones as proposed in [30] (the lower, the better).

All quantitative results are summarized in Table I. As shown in both Fig. 1 and Table I, temporal features are well-reconstructed by both methods, except for the third atom. Global reconstruction and spatial localization are significantly improved when low-rank decomposition is performed in the sensor rather than the source space, as illustrated in Fig. 2 in the iSNR = 5 dB and $w = 0.99$ scenario. One can also observe that the higher the decorrelation is, the harder it is to locate the sources precisely. From a computational point of view, the CDLFirst method converges in 585 s instead of 732 s for the IPFirst method to reach an accuracy of $\epsilon = 10^{-4}$ on the relative error averaged on the outputs. If the number of iterations is fixed to 100, CDLFirst (resp. IPFirst) computes in 137 s (resp. 212 s), with marginal differences in the quantitative results. All numerical results have been obtained on a MacBook with an Apple M1 Pro processor using MATLAB. The MATLAB code is available at the following address: https://github.com/JBMalagnoux/Code_SAMPTA.

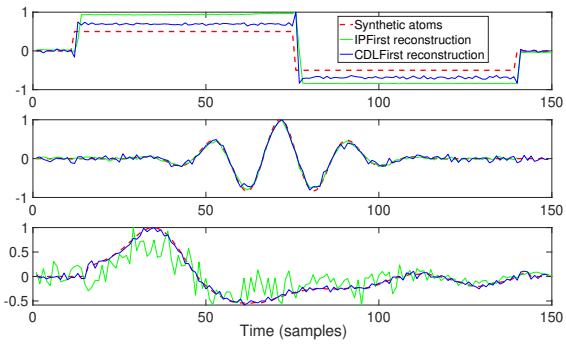

Fig. 1. Temporal patterns recovery for $w = 0.8$ and $iSNR = 5$

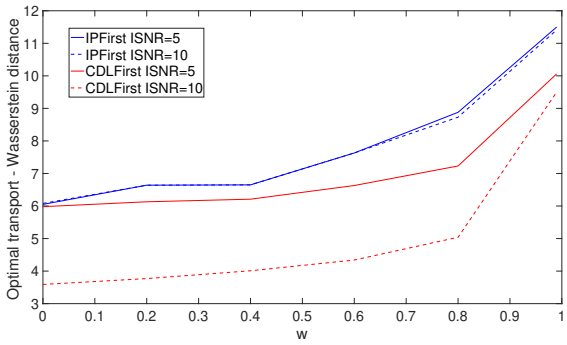

Fig. 2. Wasserstein distance on spatial dictionnary $\tilde{\mathbf{u}}$ with respect to the correlation coefficient w (the lower, the better).

V. CONCLUSION

The proposed method of applying CDL to the sensor space before addressing the inverse problem improves both computational efficiency and localization accuracy. By initially conducting CDL decomposition on the sensor data, we can effectively reduce dimensional complexity and enhance source activities' temporal and spatial localization. This approach yields superior results in source reconstruction, particularly in scenarios characterized by high data sparsity when compared to methods that tackle the inverse problem before decomposition. Future research will aim to implement this methodology with actual MEG data.

REFERENCES

[1] F. Feng, "Séparation aveugle de source : de l'instantané au convolutif," Theses, Université Paris Saclay (COmUE), Sep. 2017.

[2] Y. Song, L. Shen, L. Xing, and S. Ermon, "Solving inverse problems in medical imaging with score-based generative models," *arXiv preprint arXiv:2111.08005*, 2021.

[3] A. Jones and C. J. Taylor, "Solving inverse problems in computer vision by scale space reconstruction." in *MVA*, 1994, pp. 401–404.

[4] I. T. Jolliffe and J. Cadima, "Principal component analysis: a review and recent developments," *Philosophical Transactions of the Royal Society A: Mathematical, Physical and Engineering Sciences*, vol. 374, no. 2065, p. 20150202, 2016.

[5] H. Zou and L. Xue, "A selective overview of sparse principal component analysis," *Proceedings of the IEEE*, vol. 106, no. 8, pp. 1311–1320, 2018.

[6] M. Partridge and M. Jabri, "Robust principal component analysis," in *Neural Networks for Signal Processing X. Proceedings of the 2000 IEEE Signal Processing Society Workshop (Cat. No.00TH8501)*, vol. 1, 2000, pp. 289–298 vol.1.

[7] Y.-X. Wang and Y.-J. Zhang, "Nonnegative matrix factorization: A comprehensive review," *IEEE Transactions on Knowledge and Data Engineering*, vol. 25, no. 6, pp. 1336–1353, 2013.

[8] Y. E. Salehani and S. Gazor, "Smooth and sparse regularization for nmf hyperspectral unmixing," *IEEE Journal of Selected Topics in Applied Earth Observations and Remote Sensing*, vol. 10, no. 8, pp. 3677–3692, 2017.

[9] M. Aleksandrova, "Matrix Factorization and Contrast Analysis Techniques for Recommendation," Theses, Université de Lorraine, Jul. 2017.

[10] T. D. L. Tour, T. Moreau, M. Jas, and A. Gramfort, "Multivariate convolutional sparse coding for electromagnetic brain signals," 2018.

[11] H. Bristow, A. Eriksson, and S. Lucey, "Fast convolutional sparse coding," in *2013 IEEE Conference on Computer Vision and Pattern Recognition*, 2013, pp. 391–398.

[12] T. Tuomisto, R. Hari, and T. Katila, *Studies of auditory evoked magnetic and electric responses: Modality specificity and modelling.* Springer, 1983.

[13] O. S. Fahim Gohar Awan and A. Kiran, "Recent trends and advances in solving the inverse problem for eeg source localization," *Inverse Problems in Science and Engineering*, vol. 27, no. 11, pp. 1521–1536, 2019.

[14] A. Gramfort, D. Strohmeier, J. Haueisen, M. Hämäläinen, and M. Kowalski, "Time-Frequency Mixed-Norm Estimates: Sparse M/EEG imaging with non-stationary source activations," *NeuroImage*, vol. 70, pp. 410–422, Jan. 2013.

[15] S. R. Jones, "When brain rhythms aren't 'rhythmic': implication for their mechanisms and meaning," *Current Opinion in Neurobiology*, vol. 40, pp. 72–80, 2016.

[16] S. Cole, R. Meij, E. Peterson, C. De Hemptinne, P. Starr, and B. Voytek, "Nonsinusoidal beta oscillations reflect cortical pathophysiology in parkinson's disease," *The Journal of Neuroscience*, vol. 37, pp. 2208–16, 04 2017.

[17] C. Garcia-Cardona and B. Wohlberg, "Convolutional dictionary learning: A comparative review and new algorithms," *IEEE Transactions on Computational Imaging*, vol. 4, no. 3, pp. 366–381, 2018.

[18] K. Kavukcuoglu, P. Sermanet, Y.-L. Boureau, K. Gregor, M. Mathieu, Y. Cun *et al.*, "Learning convolutional feature hierarchies for visual recognition," *Advances in neural information processing systems*, vol. 23, 2010.

[19] B. Wohlberg, "Efficient algorithms for convolutional sparse representations," *IEEE Transactions on Image Processing*, vol. 25, no. 1, pp. 301–315, 2016.

[20] R. Grosse, R. Raina, H. Kwong, and A. Ng, "Shift-invariant sparse coding for audio classification," *Cortex*, vol. 9, 06 2012.

[21] B. Wohlberg, "Convolutional sparse representation of color images," in *2016 IEEE Southwest Symposium on Image Analysis and Interpretation (SSIAI)*, 2016, pp. 57–60.

[22] R. Hari and A. Puce, *MEG-EEG Primer*. Oxford University Press, 03 2017.

[23] B. Kong and C. C. Fowlkes, "Fast convolutional sparse coding (fcsc)," *Department of Computer Science, University of California, Irvine, Tech. Rep*, 2014.

[24] R. Tibshirani, "Regression shrinkage and selection via the lasso," *Journal of the Royal Statistical Society. Series B (Methodological)*, vol. 58, no. 1, pp. 267–288, 1996.

[25] S. S. Chen, D. L. Donoho, and M. A. Saunders, "Atomic decomposition by basis pursuit," *SIAM Journal on Scientific Computing*, vol. 20, no. 1, pp. 33–61, 1998.

[26] A. Beck and M. Teboulle, "A fast iterative shrinkage-thresholding algorithm for linear inverse problems," *SIAM Journal on Imaging Sciences*, vol. 2, no. 1, pp. 183–202, 2009.

[27] K. Miettinen, *Nonlinear multiobjective optimization*. Springer Science & Business Media, 1999, vol. 12.

[28] P. Barbault, M. Kowalski, and C. Soussen, "Parameter estimation in sparse inverse problems using bernoulli-gaussian prior," in *ICASSP 2022 - 2022 IEEE International Conference on Acoustics, Speech and Signal Processing (ICASSP)*, 2022, pp. 5413–5417.

[29] J.-B. Malagnoux and M. Kowalski, "From convolutional sparse coding to*-nmf factorization of time-frequency coefficients," in *ICASSP 2024-2024 IEEE International Conference on Acoustics, Speech and Signal Processing (ICASSP)*. IEEE, 2024, pp. 5530–5534.

[30] J. Solomon, F. de Goes, G. Peyré, M. Cuturi, A. Butscher, A. Nguyen, T. Du, and L. Guibas, "Convolutional wasserstein distances: efficient optimal transportation on geometric domains," *ACM Trans. Graph.*, vol. 34, no. 4, Jul. 2015.